Al-Furat Journal of Innovations in Electronics and Computer Engineering (FJIECE)
ISSN -2708-3985

Glaucoma Disease Diagnosis-Based Deep Learning Network

Rawa'a Humam Aziz[1*], Lamia Abed Noor Muhammed[2]

[1]University of Al-Qadisiya, College of Computer of Sciences and IT, Iraq, it.mast.23.4@qu.edu.iq
[2]University of Al-Qadisiya, College of Computer of Sciences and IT, Iraq, lamia.abed@qu.edu.iq

[*]Corresponding author E-mail: it.mast.23.4@qu.edu.iq

https://doi.org/10.46649/fjiece.v4.1.5a.25.3.2025

Abstract*. Increased intraocular pressure and optic nerve damage, which may cause irreversible blindness, are the hallmarks of glaucoma. If this disease is identified early on, its severe effects can be prevented. However, among the older population, the illness is often identified at a later stage. Consequently, individuals may be spared irreversible visual loss by early identification. Ophthalmologists use a variety of expensive, time-consuming, skill-oriented techniques when manually assessing glaucoma. A definitive diagnostic method for early-stage glaucoma detection is still elusive, while a number of approaches are in the experimental stages of development. We offer an autonomous deep learning-based technique that has very high accuracy in detecting early-stage glaucoma. The detection method entails identifying patterns in the retinal pictures that physicians frequently miss. A test accuracy of 99.26% was attained in this study using the Resnet-50 network and data from the G1020 database that had been processed and transformed from RGB to RGBA.*

Keywords*: Glaucoma; optic nerve damage; deep learning; retinal pictures.*

1. INTRODUCTION

Glaucoma, also known as the “silent thief of sight,” is the second leading cause of irreversible blindness worldwide. The disease has no obvious signs and often lasts for 10 to 15 minutes, and if left untreated, it can affect the optic nerve and cause blindness. Glaucoma is often caused by high blood pressure that affects the optic nerve and is currently the most common cause of vision loss. It causes thinning of the lower border around the optic nerve and dilation of the optic cup area, both of which are indicators of changes associated with it. [4, 12, and 15].

An anomaly in the fluid balance inside the eye causes an increase in the intraocular pressure, which damages the nerve cells and results in glaucoma, a dangerous disorder of the eyes. Impaired vision is the outcome of damaging effects on the optic nerve caused by elevated intraocular pressure (IOP). Ocular discomfort may arise from the delayed advancement of glaucoma. Other symptoms that may manifest, particularly in cases of severe IOP levels, are headache, abrupt eye pain, and halos surrounding lights. Medications and surgical procedures can be used to treat and even cure vision impairment. The early stages of glaucoma can be effectively treated with a range of surgical procedures and medication therapies. It takes longer using current approaches to achieve the most desirable results. To prevent blindness, glaucoma must be diagnosed early. Around 3.54% of people between the ages of 40 and 80 worldwide suffer from glaucoma. This means that around one in 200 people over the age of 40 may have glaucoma, and by the time they are 80 years old, that figure rises to one in eight. Elevated IOP is one of the many factors that increase the risk of glaucoma, and it plays a major role in the deterioration of optic

nerves and blood vessels. Glaucoma can cause irreversible vision loss and complete optic nerve dysfunction if left untreated. It accounts for almost 12% of all occurrences of blindness annually [6]. The projected population affected by glaucoma by 2040 is expected to be 111.8 million, with a higher prevalence among individuals between the ages of 40 and 80. In addition, data show that 4.7% of people over the age of 70 and 2.4% of the general population are susceptible to this illness [14]. A human's ocular hypertension is defined as an IOP greater than 22 mmHg [10].

The optic nerve, which transmits signals from the retina to the brain, is formed when ganglion cell axons converge at the optic disc and exit the eye. The optic cup, a structure in the center of the disc, is what gives the optic disc its distinct color. Patients with glaucoma have an increase in the size of their optic cup as a result of ganglion cell death caused by increased intraocular pressure (IOP) and/or decreased blood flow to the optic nerve. Consequently, the cup-to-disc ratio (CDR) is a crucial metric for glaucoma early identification as well as the quantitative evaluation of the condition's severity [7].

Additionally, statistics show that in the upcoming decades, there will be a rise in the number of persons experiencing eye disease, vision impairment, and blindness as a result of population expansion, aging, changes in behavior and lifestyle, and urbanization. It is important to recognize the significance of eye illnesses that typically do not result in visual impairment. However, the core of preventative and intervention methods is, understandably, eye illnesses that can result in blindness and visual impairment. Because it can result in permanent blindness, glaucoma is the most significant of these conditions. According to statistics, there are an estimated 64 million glaucoma sufferers globally, of whom 6.9 million only have moderate to severe impairment of their distant vision or blindness as a result of more severe types of the condition. Glaucoma can damage the eye's fundus, which can lead to a progressive loss of vision and, in extreme situations, blindness. Defects in the visual field are a result of the optic nerve's alterations in this disorder. Although elevated intraocular pressure (IOP), a significant risk factor, is frequently directly linked to its formation, its diagnostic use is limited due to the large number of patients who have normal-tension glaucoma. All forms of glaucoma share a gradual deterioration to the optic nerve. Most of the time, vision loss happens gradually, starting with mid-peripheral visual loss and progressing to central vision in later stages, which results in permanent blindness [5].

Soohyun Wang et al. used modified attention U-Net & EfficientNetV2 [1]. ResNet, the abbreviation for the residual network, was employed by Ayesha Shoukat et al. to tackle the vanishing gradient problem by employing the skip connection technique [2]. Gendry Alfonso-Francia et al. used Global Context Network in their research [3]. Hussein Mahdi et al. used outlined a novel automatic technique for diagnosing glaucoma that uses three different feature sets (medical, textural, and deep) to provide more information for the disease's detection. The YOLOv8 algorithm is used to identify the optic disc and cup [4]. Clerimar Paulo Braganca et al. used a mix of deep learning techniques using CNNs that have been taught for automatic glaucoma detection [5].

Three CNN architectures are proposed by Thisara et al. for attention U-Net models: Inception-V3, Visual Geometry Group 19 (VGG19), and Residual Neural Network 50 (ResNet50) for fundus picture segmentation. Data augmentation techniques were used to obtain the highest accuracy and to avoid overfitting. They recommended using the U-Net architecture along with Focus AG for each skip connection. To discover the best segmentation results, they replaced the original encoder of the standard UNet in the shrinkage path with pre-trained networks, such as VGG19, Inception-v3, and ResNet50 as baseline networks independently. These three networks use similar encoders, namely upsampling, convolution, and concatenation. The encoder merges the up-sampled output with the feature maps in the concatenation layers [15].

To replicate human classification, the researchers worked on a set of learning discriminant features and combined them for classification, where deep learning and convolutional neural networks are used in the program. It is noted that the results of the Glaucoma Net have remarkable accuracy in detecting POAG

on two datasets: the first is the Ocular Hypertension Treatment Study (OHTS) dataset and the second is the Large-scale Attention-Based Glaucoma (LAG) dataset . By tackling issues including the requirement for a variety of imaging data and a significant reliance on perimetry, the method showed increased transparency and comprehensiveness in POAG diagnosis. This study presents a public version of Glaucoma Net and demonstrates how deep learning may aid in clinical POAG detection [16].
The researchers used a computer-aided diagnostic (CAD) system that uses artificial intelligence, fundus images, and image processing techniques to identify eye conditions. To improve picture quality, the suggested method pre-processes images using a median filter and the green channel. After features are extracted using a modified convolutional neural network (CNN), the output is fed into a support vector machine (SVM) classifier for classification. The results demonstrate that the suggested CAD approach can properly classify a range of eye diseases [17].

A two-step procedure was employed by the researchers. The super pixel approach and supervised machine learning without feature selection are used in the first step. In the second step, feature selection techniques are used to boost efficiency. The assessment of the vertical cup-to-disc ratio (CDR) in retinal fundus photos as a clinical marker for glaucoma differentiation is covered [18].

2. METHODS AND MATERIALS

2.1. *Deep Learning*

In order to simulate the mechanism of the human brain, three or more layers of neural networks are used in the field of deep learning for machine learning by training huge amounts of data, but they fail to achieve its capabilities. The intelligent assumptions made by the neural network, even with a single layer, can enhance the network and improve its accuracy with the help of additional hidden layers. Through the services and applications provided by artificial intelligence that increase automation in performing analytical and physical activities without human interaction through deep learning. [14].

Tens or even hundreds of layers make up a convolutional neural network, and each layer is taught to recognize a unique aspect of an image. The result of each convolved image serves as the layer's input after each training image has been filtered at a different resolution. The filters can start with very simple standards like brightness and edges and go more sophisticated by adding features that uniquely identify the object. Recent work has shown that deep learning algorithms can provide highly representations, which have proven useful in a variety of computer vision tasks [9].

2.2. Transfer Learning

Transfer learning is a machine learning technique in which a pre-trained model is modified to carry out a similar task on a new dataset. Usually, the model has been trained on a big dataset. This method makes use of the pre-training knowledge that the model acquired to enhance performance and shorten the training duration for the new assignment. Utilizing a pre-trained model allows one to benefit from the edges, textures, and forms that the model has previously learnt. These features are frequently applicable to many applications and datasets.

The development of artificial intelligence could aid in the quick and precise detection of illnesses. The robust image classification architecture of ResNet-50 is utilized in the development of the suggested model. Since fundus imaging accurately portrays the inside structure of the eye, it is utilized, and Fig.1. shows the architecture of ResNet-50 [2]. ResNet-50, the least complex model, extracts accurate features with nearly perfect outcomes [3, 13].

Al-Furat Journal of Innovations in Electronics and Computer Engineering (FJIECE)
ISSN -2708-3985

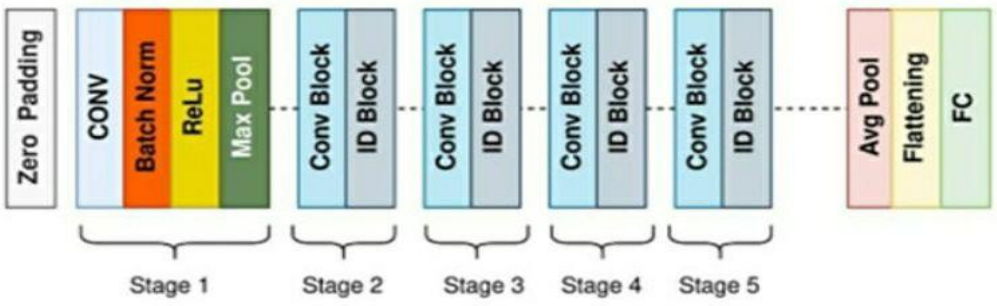

Fig. 1. Block diagram of ResNet-50 architecture [2]

2.3. *RGBA*

In order to facilitate the identification of the typical thinning of the optic nerve bundles associated with glaucoma, color palettes were employed. The images were converted from an RGB three-channel data format to an RGBA four-channel format in order to show brightness. After that, they were converted to grayscale and painted using several color schemes. Several adjustments were made using the different palettes available in the computer vision picture library. In the end, ophthalmologists selected five different palettes after a review and verification procedure. These included the binary series (BinaryR), the blue series (Bone, Mako, and Jet), and the red series (Gist-Heat). These palettes enable the clear observation of the structural characteristics, just how OCT equipment is used to measure the thickness of the optic nerve bundles [1]. As below in Fig. 2.

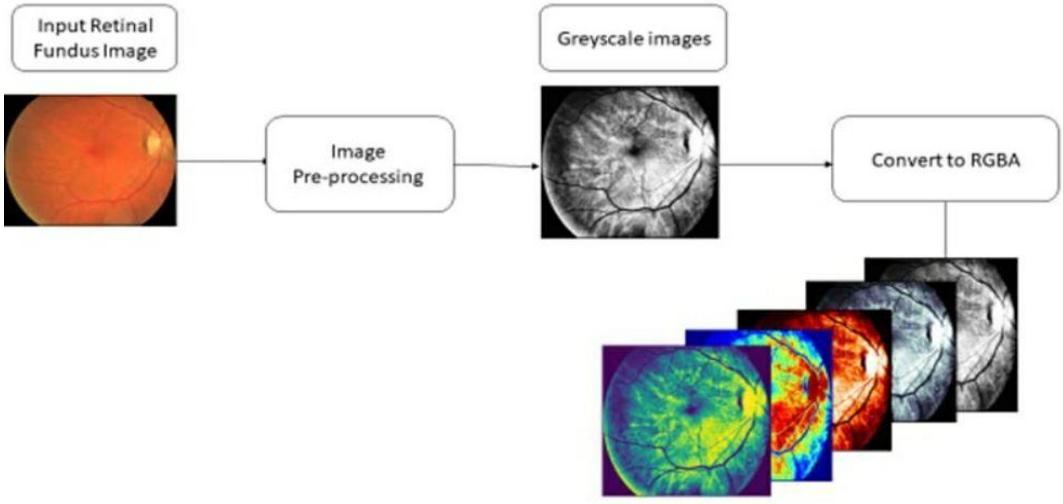

Fig. 2. Flow diagram of the preprocessing image

3. PROPOSED WORK

The G1020 Dataset was gathered between 2005 and 2017 at a private medical facility in Kaiserslautern, Germany. It is composed of 1020 retinal fundus images with great quality. There are 724 healthy photos and 296 glaucomatous images in it. The dataset offers JSON files with OC and OD ground

Al-Furat Journal of Innovations in Electronics and Computer Engineering (FJIECE)
ISSN -2708-3985

truth annotations [8, 9]. The vanishing gradient problem is resolved by the ResNet, short for residual network, which employs the skip connection method. Prior to ResNet, issues with network degradation were brought on by deeper networks. This degradation led to an increase in training error. The ResNet architecture uses the skip connection technique to get around this issue. This architecture is easier to tune, requires less training time, and exhibits higher detection accuracy. Numerous applications for image processing and illness diagnosis in the medical industry make use of the ResNet architecture. The proposed method shown below in fig. 3.

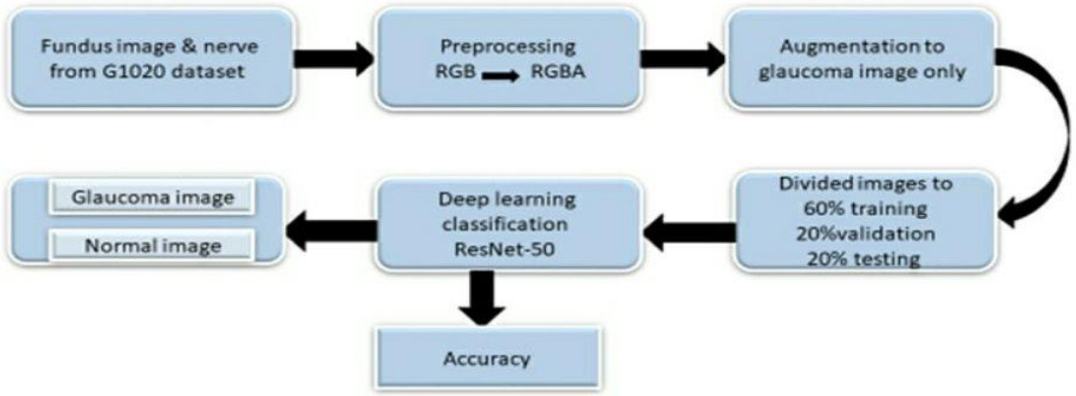

Fig. 3. Block Diagram of the Proposed Method

The ResNet-50 network is trained by loading photos from the database, analysing the data, and converting the RGB to RGBA format, as shown in the above figure. Only the data pertaining to glaucoma is then subjected to data augmentation. After then, the data is separated into three categories: 60% training, 20% validation, and 20% test. Following training, testing, and categorization of the data into impacted and unaffected categories, the network's classification accuracy is reported.

4. RESULTS AND DISCUSION

When implementing the program using database images without using any pre-processing of the images, the implementation results were very low. There are a number of reasons for this subpar performance, including possible noise in the photos and class imbalance in the data.

When enlarging the images used using augmentation, the accuracy increased slightly. When images were used after pre-processing them and converting them from RGB to RGBA format without using data stabilization or augmentation, the test accuracy also increased by a small percentage.

The test accuracy improved significantly to 0.9887 at 30 epochs after performing preprocessing, which involved converting the images from RGB to RGBA and balancing the infected images. Test accuracy increased slightly more to 0.9911 after training the model for an additional 100 epochs. The model used for training was the ResNet-50 network, all of the words mentioned in the above paragraph were explained in Figure 4.

The raw data quality was greatly improved after pre-processing, which involved transforming the photos from RGB to RGBA. This conversion helps retain more information about the photographs and improves the model's ability to discriminate between shots that are affected and those that are not.

Al-Furat Journal of Innovations in Electronics and Computer Engineering (FJIECE)
ISSN -2708-3985

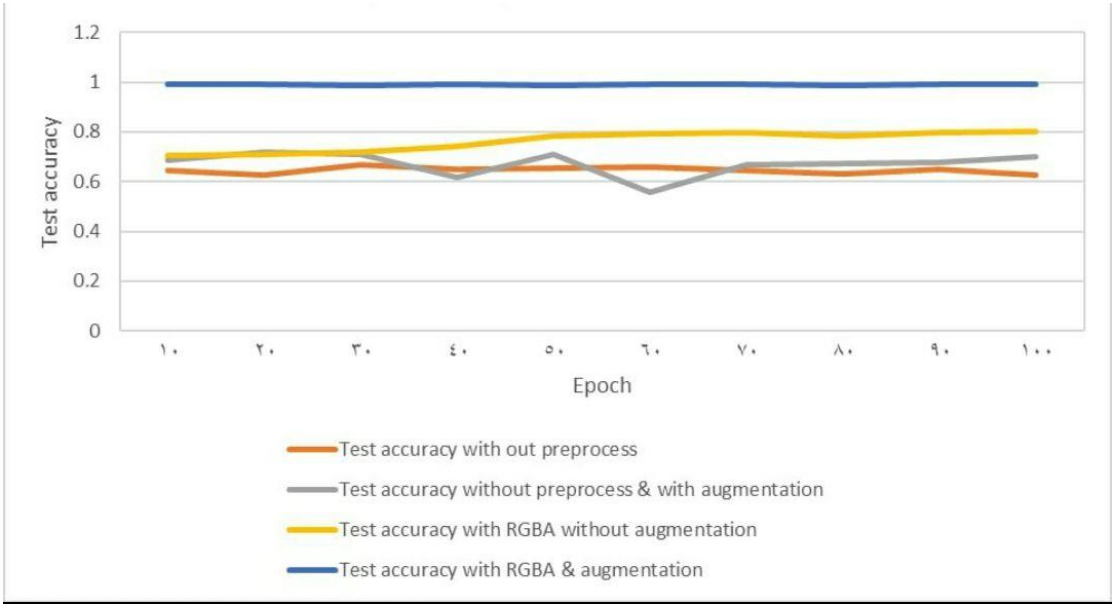

Fig. 4. Implementation Results

Additionally, by employing data augmentation techniques to balance the affected photographs, the class imbalance issue was resolved and the model was able to learn from a bigger and more representative dataset. By increasing training to 100 epochs, the model was able to refine its learning even further, leading to a little increase in test accuracy to 0.9912. This increase, however little, shows that the model continues to improve when additional training epochs are added, hence increasing its ability to generalize to new data. Despite the little increase in accuracy, the model could be approaching its performance ceiling, which is the point at which more training yields diminishing gains. Accuracy is greatly increased by pre-processing and data balancing, highlighting the importance of these processes for deep learning model training, particularly for medical image analysis. As seen in Table 1, these techniques enhance the model's capacity for learning while ensuring that the performance metrics accurately reflect the model's competence in real-world applications.

Table 1. Accuracy Table in Different Type of Method.

Method type	Best value of accuracy	Average accuracy for different tests
Accuracy without preprocessing & without augmentation	0.666666687	0.646078444
Accuracy without preprocessing & with augmentation	0.72058821	0.67230392
Accuracy with preprocessing & without augmentation	0.801587284	0.763219249
Accuracy with preprocessing & with augmentation	0.992647	0.990196

Overall, the results demonstrate that proper data pre-processing and balancing are necessary to optimize model performance, especially in medical image analysis applications where data representation and quality are crucial. Future studies should look at novel pre-processing techniques and data augmentation strategies to further increase the model's accuracy and resilience.

Table 2. Comparison the Proposed Models with Other Works.

Author	Year	Dataset	Technique	Accuracy
Farheen Chincholi et al [12]	2024	G1020	DETR	90.48%
Debendra Muduli et al [19]	2024	G1020	FDCT-WRP, MOD-POA-ELM	93.25%
M.Shanmuga Eswari et al [20]	2024	G1020	TernausNet	94.5%
Proposed method	2024	G1020	RGBA + ResNet-50	99.26%

5. CONCLUSION

A systematic pre-processing and analysis of fundus images from the G1020 dataset is used in the proposed glaucoma detection approach. The RGB to RGBA format conversion is done on the images during the first pre-processing stage. This step most often include adding an alpha channel to allow for more intricate picture manipulation. Data augmentation is only used on glaucoma pictures following pre-processing to account for any class imbalances in the dataset. This provides a neutral evaluation of the model's performance on unseen data. Renowned for its robustness in image recognition applications, the convolutional neural network ResNet-50 is a popular model for deep learning categorization. The technique feeds the pre-processed and enriched photos into the ResNet-50 model in an effort to accurately discriminate between normal and glaucoma images. Finally, the method evaluates the classification accuracy, providing a numerical depiction of the model's effectiveness in detecting glaucoma. This systematic approach highlights the importance of balanced pre-processing, data augmentation, and data partitioning to develop a reliable deep learning model for medical picture categorization.

REFERENCES

[1] S. Wang, B. Kim, J. Kang, and D. S. Eom, “Precision Diagnosis of Glaucoma with VLLM Ensemble Deep Learning,” *Appl. Sci.*, vol. 14, no. 11, 2024, doi: 10.3390/app14114588.

[2] A. Shoukat, S. Akbar, S. A. Hassan, S. Iqbal, A. Mehmood, and Q. M. Ilyas, “Automatic Diagnosis of Glaucoma from Retinal Images Using Deep Learning Approach,” *Diagnostics*, vol. 13, no. 10, pp. 1–17, 2023, doi: 10.3390/diagnostics13101738.

[3] G. Alfonso-Francia *et al.*, "Performance Evaluation of Different Object Detection Models for the Segmentation of Optical Cups and Discs," *Diagnostics*, vol. 12, no. 12, 2022, doi: 10.3390/diagnostics12123031.
[4] H. Mahdi and N. El Abbadi, "Tri-AlgoVision: A Multifaceted Approach for Automated Glaucoma Diagnosis," *Int. J. Intell. Eng. Syst.*, vol. 16, no. 6, pp. 433–444, 2023, doi: 10.22266/ijies2023.1231.36.
[5] C. P. Bragança, J. M. Torres, C. P. de A. Soares, and L. O. Macedo, "Detection of Glaucoma on Fundus Images Using Deep Learning on a New Image Set Obtained with a Smartphone and Handheld Ophthalmoscope," *Healthc.*, vol. 10, no. 12, 2022, doi: 10.3390/healthcare10122345.
[6] M. Vadduri, "ENHANCING GLAUCOMA DIAGNOSIS : DEEP LEARNING MODELS FOR AUTOMATED IDENTIFICATION AND," vol. 102, no. 13, pp. 5346–5363, 2024.
[7] S. Tadisetty, R. Chodavarapu, R. Jin, R. J. Clements, and M. Yu, "Identifying the Edges of the Optic Cup and the Optic Disc in Glaucoma Patients by Segmentation," *Sensors*, vol. 23, no. 10, 2023, doi: 10.3390/s23104668.
[8] J. Sigut, F. Fumero, J. Estévez, S. Alayón, and T. Díaz-Alemán, "In-Depth Evaluation of Saliency Maps for Interpreting Convolutional Neural Network Decisions in the Diagnosis of Glaucoma Based on Fundus Imaging," *Sensors*, vol. 24, no. 1, 2024, doi: 10.3390/s24010239.
[9] H. Fu, J. Cheng, Y. Xu, and J. Liu, "Glaucoma Detection Based on Deep Learning Network in Fundus Image," *Adv. Comput. Vis. Pattern Recognit.*, no. November, pp. 119–137, 2019, doi: 10.1007/978-3-030-13969-8_6.
[10] D. J. Nam, "Distributed Glaucoma Detection Method Using Privacy- Preserving Federated Learning," 2024, doi: 10.36838/v6i1.4.
[11] M. N. Bajwa, G. A. P. Singh, W. Neumeier, M. I. Malik, A. Dengel, and S. Ahmed, "G1020: A Benchmark Retinal Fundus Image Dataset for Computer-Aided Glaucoma Detection," *Proc. Int. Jt. Conf. Neural Networks*, 2020, doi: 10.1109/IJCNN48605.2020.9207664.
[12] F. Chincholi and H. Koestler, "Transforming glaucoma diagnosis: transformers at the forefront," *Front. Artif. Intell.*, vol. 7, 2024, doi: 10.3389/frai.2024.1324109.
[13] T. Shyamalee and D. Meedeniya, "Glaucoma Detection with Retinal Fundus Images Using Segmentation and Classification," *Mach. Intell. Res.*, vol. 19, no. 6, pp. 563–580, 2022, doi: 10.1007/s11633-022-1354-z.
[14] R. Kashyap, R. Nair, S. M. P. Gangadharan, M. Botto-Tobar, S. Farooq, and A. Rizwan, "Glaucoma Detection and Classification Using Improved U-Net Deep Learning Model," *Healthc.*, vol. 10, no. 12, 2022, doi: 10.3390/healthcare10122497.
[15] T. Shyamalee and D. Meedeniya, "Attention U-Net for Glaucoma Identification Using Fundus Image Segmentation," *2022 Int. Conf. Decis. Aid Sci. Appl. DASA 2022*, no. May, pp. 6–10, 2022, doi: 10.1109/DASA54658.2022.9765303.
[16] M. Lin *et al.*, "Automated diagnosing primary open-angle glaucoma from fundus image by simulating human's grading with deep learning," *Sci. Rep.*, vol. 12, no. 1, pp. 1–11, 2022, doi: 10.1038/s41598-022-17753-4.
[17] A. Zyout, H. Alquran, W. A. Mustafa, M. Alsalatie, A. Al-Badarneh, and W. Khairunizam, "Automated Diagnosis of Eye Fundus Images," *Proc. Int. Conf. Artif. Life Robot.*, pp. 56–61, 2023, doi: 10.5954/icarob.2023.os1-7.
[18] O. M. Kamara, A. H. Asad, and H. A. Hefny, "Automated Diagnoses Glaucoma Approach in Retinal Fundus Images Using Support Vector Machine," *Lect. Notes Data Eng. Commun. Technol.*, vol. 184, pp. 368–379, 2023, doi: 10.1007/978-3-031-43247-7_33.
[19] Debendra Muduli, Rani Kumari, Adnan Akhunzada, Korhan Cengiz, Santosh Kumar Sharma, Rakesh Ranjan Kumar & Dinesh Kumar Sah," Retinal imaging based glaucoma detection using

modified pelican optimization based extreme learning machine," Scientific Reports volume 14, Article number: 29660 (2024).

[20] M Shanmuga Eswari, S Balamurali, Lakshmana Kumar Ramasamy," Hybrid convolutional neural network optimized with an artificial algae algorithm for glaucoma screening using fundus images," PMID: 39301801 PMCID: PMC11539265 DOI: 10.1177/03000605241271766.

[21] Debendra Muduli, Harald Koestler, "Transforming glaucoma diagnosis: transformers at the forefront," Front Artif Intell. 2024 Jan 15;7:1324109. doi: 10.3389/frai.2024.1324109.